

Fuzzy inference petri net modelling and state flow simulation for quality anomaly monitoring and diagnosis

Shiwang Hou^{1,*}, and Zhuoyang Li²

¹Business School, Huaihua University, Huaihua 418000, China

²School of Economics and Management, North University of China, Taiyuan 030051, China

Abstract. Fuzzy Reasoning Petri Nets (FRPNs) are highly suitable for diagnosing quality anomalies in uncertain scenarios. However, the unique graphical representation and complex logical structure of FRPNs pose challenges for traditional Petri net simulation methods, limiting the ability to effectively model FRPNs and hinder dynamic analysis of anomaly generation and propagation through simulation. This paper introduces a Stateflow-based modelling and simulation approach for FRPNs, utilizing elements from the Stateflow diagram, including state, transition, state action, and transition labels. These elements are used to represent the position, directed arcs, and transition rules of FRPNs. By incorporating transition relationships and monitoring logic, a Stateflow based simulation model of FRPNs is constructed. This model takes control chart data as input, dynamically analyses the occurrence level of abnormal patterns in the control chart, providing a demonstration of the diagnostic process and ultimately delivering a diagnostic outcome.

1 Introduction

Control charts, a key tool in Statistical Quality Control (SQC), are extensively utilized for monitoring process stability and capability. They utilize measurements of one or multiple quality-related characteristics of the manufacturing process as operational parameters, distinguishing normal fluctuations from abnormal ones through control limits and statistical tests. Control charts are generated based on quality characteristic data sampled at different time intervals. An anomaly refers to a non-statistically normal state that occurs in the quality control of the manufacturing process. When anomalies occur, typical process signals are often composed of multiple frequency components, leading to various abnormal patterns in the control charts. Each pattern signifies different underlying abnormal factors in the process and usually holds significant physical meaning. These patterns often indicate different causes of process instability in specific application scenarios.

The objective of anomaly diagnosis is to analyse the cause-effect relationship between states and identify the root causes of abnormalities. Modelling and simulating quality

* Corresponding author: houshiwang@nuc.edu.cn

diagnosis are essential for validating the accuracy of the diagnostic process and demonstrating its dynamic nature. However, the manufacturing quality control process involves substantial uncertain information, including the randomness of anomaly occurrences, the vagueness of abnormal symptoms, and the uncertainty, inconsistency, and incompleteness of experiential knowledge in diagnosis. Properly describing and incorporating these types of information is crucial for modelling and simulating the quality diagnosis process. Fuzzy production rules, when applied to fuzzy Petri nets, effectively handle fuzzy uncertain information through the mapping of fuzzy rules to structured knowledge representations. Additionally, fuzzy Petri nets possess fuzzy inference capabilities similar to fuzzy systems, thereby facilitating knowledge analysis, reasoning, testing, and decision support.

Fuzzy Reasoning Petri Nets (FRPNs) have gained significant attention and are widely studied in dealing with vague or fuzzy information. Researchers have recognized FRPNs as a valuable model for representing and reasoning with fuzzy knowledge within knowledge-based systems. In reference [1], a model based on FRPNs was utilized to represent the fuzzy production rules within a rule-based system. This model effectively captures expert knowledge and facilitates fuzzy reasoning. A knowledge representation model, designed with the capability to adapt to information dynamics, was developed to address the challenges posed by vague and fuzzy information in complex product design [2]. The proposed model combines the characteristics of a fuzzy Petri net with the learning ability of evolutionary algorithms. In [3], a novel model for fault diagnosis and cause analysis was presented, utilizing a fuzzy evidential reasoning approach combined with a dynamic adaptive fuzzy Petri net. This model addresses both forward fault diagnosis and backward cause analysis.

A dynamic reasoning system based on adaptive fuzzy higher-order Petri nets was proposed in [4]. The proposed model allows for adjusting the arc weights to accommodate changes in the system across various application domains. A hybrid approach leveraging a generalized fuzzy event-condition-action rule and a typed fuzzy Petri net extended with process knowledge was proposed in reference [5]. This approach enables the integrated representation and reasoning of both fuzzy and non-fuzzy knowledge, as well as specific application domain knowledge and workflow process knowledge. A specific type of timed fuzzy Petri net was developed for knowledge representation of chemical abnormalities in [6]. This model incorporates timing factors assigned to each transition and reliability degrees associated with each place, allowing for accurate representation of the dynamic nature of fuzzy knowledge concerning abnormal events. Reference [7] and [8] proposed that the Fuzzy Petri net, based on fuzzy production rules, effectively represented and handled ambiguous knowledge. This model reasons based on the confidence of each transition and identifies the causes of failures. However, as the size of the model increases, implementing inference using the Fuzzy Petri net becomes more challenging. In response to this issue, Reference [9] introduced a decomposition algorithm to address the problem of state space explosion when applying fuzzy Petri nets. In order to enhance the knowledge representation and reasoning capabilities of FRPNs in large-scale collective environments, a grey reasoning Petri net (GRPNs) was proposed in reference [10]. It aims to simulate grey generation rules in expert systems and introduces a largescale collective decision-making method based on grey correlation analysis to obtain the knowledge parameters of the GRPN model.

Also, it has been used in modelling and analysing fault diagnosis systems for gas turbines(see [11]), CNC machine tools(see [12]), communication safety (see [13]), power system(see[14]), biological systems(see [15]) and manufacturing systems(see [16] [17] [18][19]). All above literatures obtained the results based on arithmetical operation. In order to validate the running process and reasoning result of the FRPNs model dynamically,

appropriate simulating tools must be adopted. For its particular graphic representation and logic structure, traditional Petri net software, such as PNK([20]), CPN([21]) and Visual Object Net++([22]), is hard to simulate and analyse its performance. Stateflow is a graphic tool of finite state machine to modelling discrete event system and has been used to simulating Petri net (such as[23][24][25][26]). By modifying aforementioned methods and adding presentation mechanism for fuzzy elements, Stateflow can be used to simulate event-driven based FRPNs model.

The purpose of this paper is to develop a FRPNs model for diagnosing uncertain quality anomalies and proposes a detailed scheme for simulating this model by use of Stateflow. The remaining sections of the paper are organized as follows. Section 2 gave definitions for the non-deterministic quality anomaly patterns discussed in this paper, along with the measurement methods used to quantify their individual occurrence degree. Section 3 presented the method for representing uncertain quality anomaly diagnostic rules using FRPNs, along with the simulation method of FRPNs using Stateflow. In conclusion, Section 4 concluded the paper and offered some suggestions for future research.

2 Definition and measurement of non-deterministic quality anomaly patterns

2.1 Definition of non-deterministic quality anomaly patterns

The criteria for a manufacturing process to be considered in control generally require that the points on the control chart remain within the control limits and exhibit no statistical defects in their arrangement and distribution. These defects, also referred to as abnormal patterns on the control chart, encompass various situations such as runs, shifts, trends, cycles, proximities, stratifications, abrupt changes, and mixed distributions, each characterized by distinct features. The most commonly employed approach involves applying specific statistical criteria to identify these patterns. For instance, a consecutive run of 7 points showing a consistent increase or decrease signifies a trend abnormal pattern. Different discernment rules may be employed depending on the specific application context.

The six major factors, i.e. 5M1E—manpower, machines, materials methods, measurements, and environment—in the manufacturing process constitute a complex system, characterized by the dynamic generation and propagation of anomalies. The occurrence of an abnormal state can trigger a cascade of subsequent states, resulting in concurrent anomalies. An anomaly can be attributed to multiple causes, with different primary anomalies following distinct propagation pathways but ultimately leading to the same system-level anomaly. Consequently, when utilizing control charts for process anomaly pattern recognition and diagnosis, the following uncertainties arise: (1) data points fall on or near the control lines or boundaries, (2) the number of abnormal data points is in close proximity to the specified threshold, (3) diagnosing the causes of abnormalities when a specific point on the control chart triggers two or more abnormal patterns simultaneously, and (4) classification and identification of abnormal patterns, along with the determination of their respective causes in situations involving the concurrent presence of multiple quality anomalies.

To address aforementioned non-deterministic issues, this study examined five categories of abnormal patterns within the context of control charts. The OCL pattern is identified when data points on the control chart surpass the ± 3 standard deviation limit lines. The Freak pattern manifest when two or more points fall within the range of 2σ to 3σ , or -3σ to -2σ , in a sequence of three consecutive points on the control chart. The Shift pattern characterize a scenario where the process mean deviates from the target mean. The

Trend pattern is discerned through the occurrence of consecutively upward or downward points among seven consecutive sample points on the control chart. Lastly, the Cycle pattern occurs when plotted points on a control chart exhibits periodic variations.

2.2 Measurement of non-deterministic quality anomaly patterns

To quantitatively describe the degree of occurrence of each abnormal pattern on the control chart at each moment, this paper first calculated the corresponding characteristic numbers for the above five patterns, and then converted the characteristic numbers into the occurrence degree of abnormal patterns based on their specific membership functions.

The characteristic number of out of control limit, represented as C_{OCL} , can be calculated using the following formula

$$C_{OCL} = \frac{\bar{x}_i - \mu}{s} \tag{1}$$

where \bar{x}_i represents the sample mean corresponding to the i th point on the control chart, μ and s respectively represent the population mean and standard deviation of the monitored statistic.

The characteristic number C_F of Freak pattern can be obtained using the following equation.

$$C_F = \max \left\{ \sum_{i=k}^{k+3} I(2\sigma < x_i < 3\sigma), \sum_{i=k}^{k+3} I(-3\sigma < x_i < -2\sigma) \right\} \tag{2}$$

where $I(\cdot)$ is an indicator function, which results in 1 when the condition is satisfied and 0 otherwise.

$$I(x) = \begin{cases} 1, & \text{if } x \text{ is true} \\ 0, & \text{otherwise} \end{cases} \tag{3}$$

For the shift mode, the process mean was represented by the average of the 20 historical sample data up to the current time. The calculation method for the characteristic number C_S was as follows.

$$C_S = \frac{|\mu - \bar{x}_i|}{s} \tag{4}$$

where μ and s represented the target value and standard deviation of process, \bar{x}_i denoted the process mean from time $(i-19)$ till i , i.e.

$$\bar{x}_i = \frac{1}{20} \sum_{k=i-19}^i \bar{x}_k \tag{5}$$

For Trend and Cycle analysis, the adopted approach was as follows: Firstly, by selecting specific wavelet basis functions and determining decomposition levels, the control chart signal underwent decomposition into a series of wavelet coefficients. Subsequently, appropriate wavelet coefficients were selected for the reconstruction of control chart mode signals. The largescale approximation component A represented the low-frequency segment, denoted as the Trend mode, while the detail component D represented the high-frequency segment, identified as the Cycle mode. Finally, parameter fitting was applied to the reconstructed signals A and D, characterizing the Trend and Cycle modes, respectively. The goodness of fit served as the feature number for the corresponding abnormal modes.

For the analysis of Trends and Cycles, the adopted approach is outlined as follows: Initially, through the selection of specific wavelet basis functions and decomposition levels, the control chart signal undergoes decomposition into a series of wavelet coefficients. Subsequently, appropriate wavelet coefficients are chosen to reconstruct the control chart mode signals. Finally, parameter fitting is employed on the reconstructed signals, which

represent the Trend and Cycle modes. Goodness of fit serves as the feature number for the corresponding abnormal modes.

Using the Matlab wavelet toolbox, different wavelet functions and decomposition levels were compared for their reconstruction and fitting effects. The experimental results showed that the wavelet function *sys4* and a decomposition level of 5 yield the best performance. As shown in Fig.1., from top to bottom, they represented the original control chart signal, A5, D5, D4, D3, D2, and D1, respectively. Fig.2. represented the signal reconstructed using different wavelet coefficients. The signal reconstructed by A5 provided the best fit for the Trend pattern of the control chart, while the signal reconstructed by D4 showed the best fit with the Cycle pattern of the control chart compared to the original data.

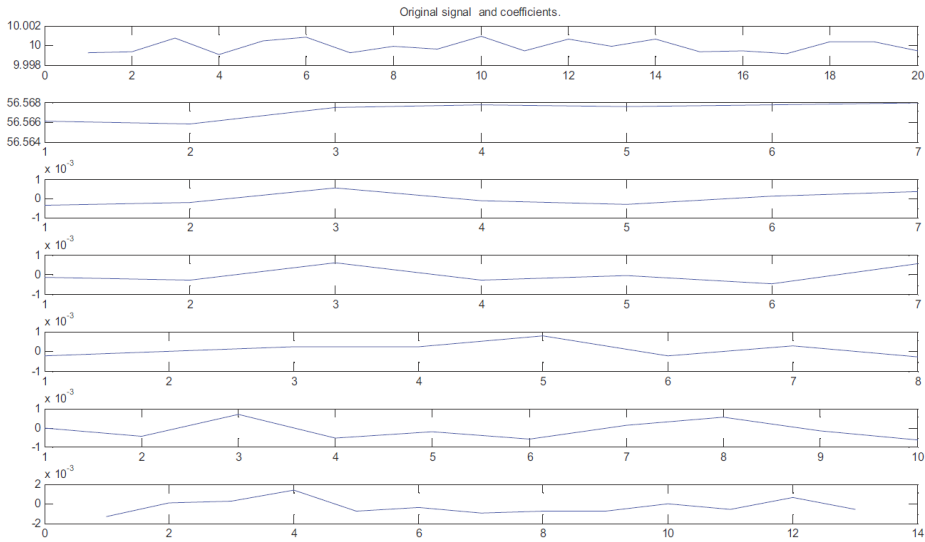


Fig. 1. Five-Level Wavelet Decomposition Coefficients of control chart.

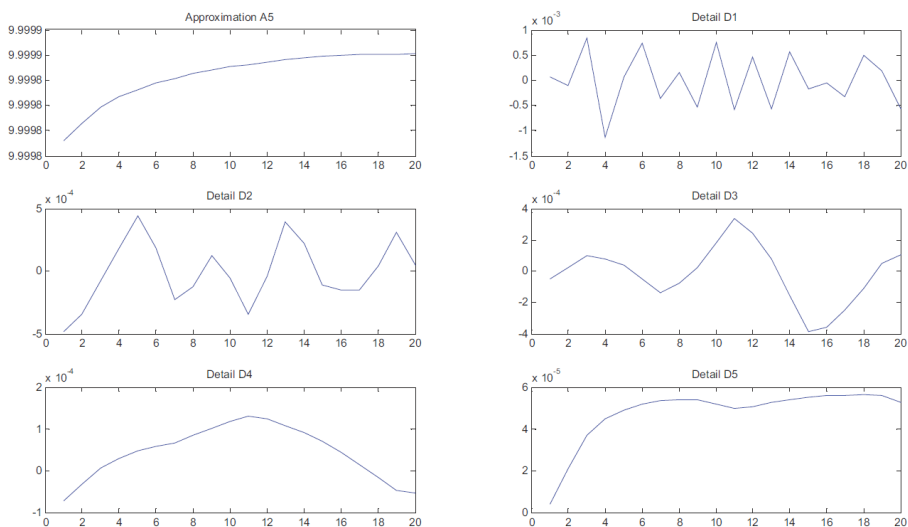


Fig. 2. Signal Reconstructed from Five-Level Wavelet Coefficients.

From the definition of the five abnormal patterns mentioned above, it is evident that they do not require the same window size. In this paper, a maximum window size of 20 was used as the warm-up period, which means that the identification and diagnosis of quality anomalies start from $i=20$. From this point onwards, samples within the required window size for each pattern were traced back, and their respective feature numbers were calculated. Afterward, the calculation is rolled forward point by point. After obtaining the characteristic numbers for each pattern, they can be transformed into the occurrence degrees of the respective patterns using the membership function. This paper adopted the following trapezoidal membership function consistently.

$$f(x, a, b, c, d) = \begin{cases} 0, & x \leq a \\ \frac{x-a}{b-a}, & a \leq x \leq b \\ 1, & b \leq x \leq c \\ \frac{d-x}{d-c}, & c \leq x \leq d \\ 0, & x \geq d \end{cases} \quad (6)$$

3 Fuzzy production rules for quality abnormality diagnosis and their presentation with FRPNs

3.1 Quality abnormality diagnosis principle of FRPNs and its stateflow modelling

Given the uncertainties, asynchrony, concurrency, and intricate causality inherent in diagnosing and disseminating uncertain quality abnormalities, FRPNs articulate fuzzy knowledge for quality control through fuzzy rules. Connections are established among rule elements, antecedents, consequents, FRPNs attributes, confidence levels, and state transitions. Rules for diagnosing quality abnormalities are represented in FRPNs, triggering transitions based on changes in antecedent states. Fuzzy membership degrees of consequent states determine contribution degrees of potential causes. Diagnostic outcomes help quality engineers promptly identify and resolve abnormalities.

States and transitions served as fundamental components within the Stateflow chart framework of the MATLAB Stateflow Toolbox. In this context, a 'State' was visually represented as a block diagram, comprising four distinct actions: 'entry', 'during', 'exit' and 'on event name'. These actions signified specific behaviours related to entering, enduring, exiting, and responding to particular events while in the state, respectively.

A 'Transition' is depicted with array lines, following the label format: 'event /[condition] condition action /transition action'. The 'event' triggers the transition, conditioned by the true specified condition. If no event is specified, the transition occurs upon any event. 'Condition' is a Boolean expression validating the transition. 'Condition action' executes immediately when the condition is true, preceding the validity determination of the transition destination. If no explicit condition is stipulated, an implicit true condition is assumed. The 'transition action' executes after the validity of the destination is confirmed, provided the condition holds true. For transitions with multiple segments, the transition action executes only when the entire path to the final destination is confirmed as valid.

Adhering to these modelling guidelines, FRPNs can be effectively modelled utilizing stateflow elements. The input places of a transition were symbolized by a cluster of concurrent superstates. Each superstate contained two mutually exclusive states, 'Normal' and 'Abnormal' to indicate the current process state. The transition between these states

depended on the truth degree of the place. Upon the occurrence of a transition between these states, the state entry action denoted as 'En' was executed. Simultaneously, the state attribute assumed a value equal to the truth degree of the place, and event 'E' was triggered in parallel.

Similarly, the output places of the transition were represented by a set of concurrent superstates, each comprising two exclusive states: 'None' and 'On' signifying the presence or absence of an assignable cause, respectively. Event 'E' assumed the role of the transition trigger between these two states within each superstate. The logical expression of the input state governed the transition condition. Lastly, the 'rule confidence' value was assigned during the 'transition action' phase.

These above-mentioned conventions and components have facilitated a structured and comprehensive modelling approach for FRPNs within the stateflow framework.

3.2 Quality abnormality diagnosis rules, its FRPNs presentation and stateflow Modelling

Let θ_i represent the truth degree of the precondition place or result place in fuzzy rule R_i , and let CL_i denote the confidence level of the fuzzy rule. The following section outlined four common types of fuzzy production rules used during the process of quality anomaly diagnosis, along with their corresponding FRPNs and stateflow models.

$$(1) R_i(CL_i) : \text{if } \theta_1(\theta_1) \text{ and } \theta_2(\theta_2) \text{ and } \dots \text{ and } \theta_{k-1}(\theta_{k-1}) \text{ then } \theta_k(\theta_k)$$

where $\theta_k = \min(\theta_1, \theta_2, \dots, \theta_{k-1}) * CL_i$. Fig. 3. showed the Petri net model and Stateflow model of this rule.

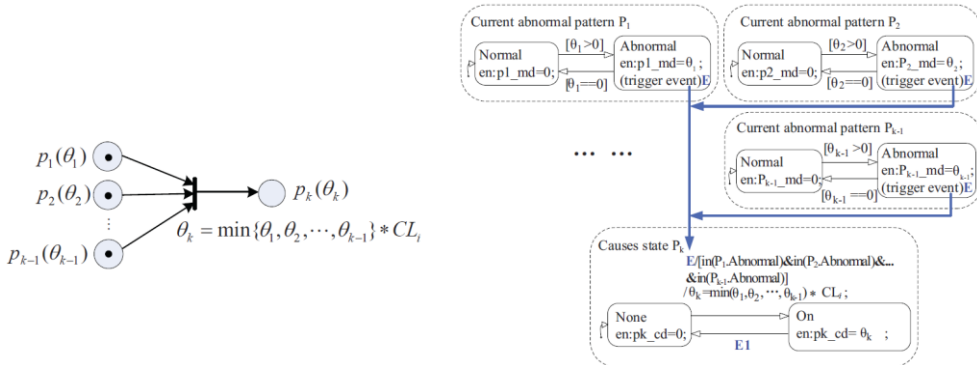


Fig. 3. The Petri net model and its Stateflow model of Type I rule.

$$(2) R_i(CL_i) : \text{if } \theta_1(\theta_1) \text{ then } \theta_2(\theta_2) \text{ and } \dots \text{ and } \theta_k(\theta_k)$$

where $\theta_j = \theta_1 * CL_i (j = 2, 3, \dots, k)$. The Petri net model and Stateflow model of this type of rule were depicted in Fig.4.

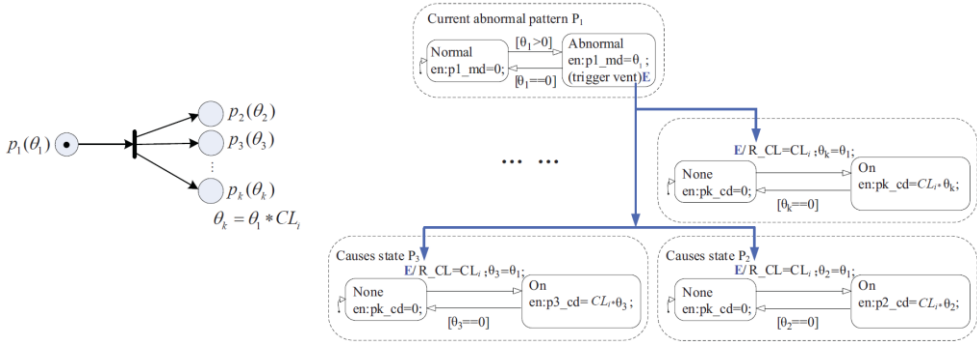


Fig. 4. The Petri net model and its Stateflow model of Type II rule.

$$(3) R_i(CL_i) : \text{if } \check{\Phi}_1(\theta_1) \check{\Delta} r \check{\Phi}_2(\theta_2) \check{\Delta} r \check{\Delta} \cdot \check{\Delta} r \check{\Phi}_{k-1}(\theta_{k-1}) \check{\Delta} \text{then } \check{\Phi}_k(\theta_k).$$

where $\theta_k = \max(\theta_1, \theta_2, \dots, \theta_{k-1}) * CL_i$. The Petri net model and Stateflow model of this type of rule were shown in Fig.5.

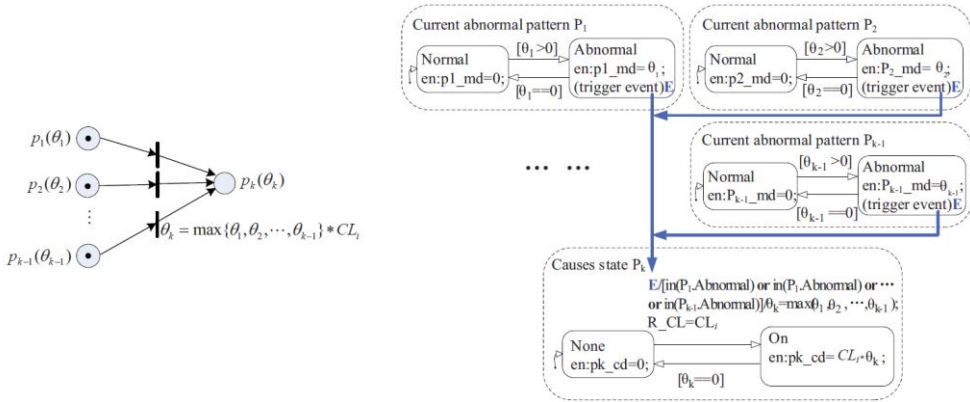


Fig. 5. The Petri net model and its Stateflow model of Type III rule.

$$(4) R_i(CL_i) : \text{if } \check{\Delta} \text{ot } \check{\Phi}_1(\theta_1) \check{\Delta} \text{then } \check{\Phi}_2(\theta_2), \text{ where } \check{\Delta} \theta_2 = (1 - \theta_1) * CL_i$$

Regarding negative propositions, they can be transformed into positive propositions through the complement operation of the place truth degree. Fig.6. illustrated the Petri net model and its Stateflow model for negative rules.

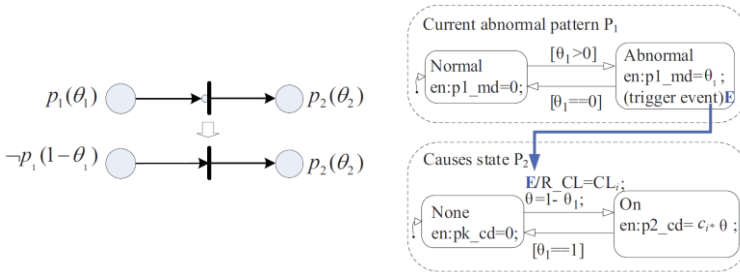


Fig. 6. The Petri net model and its Stateflow model of negative rules.

Although it is possible for rules like the following to exist, $R_i(CL_i) : \text{if } \check{\Phi}_1(\theta_1) \check{\Delta} \text{then } \check{\Phi}_2(\theta_2) \check{\Delta} r \check{\Delta} \cdot \check{\Delta} r \check{\Phi}_k(\theta_k)$, where

$\theta_j = \theta_1 * CL_i (j = 2, 3, \dots, k)$, they cannot provide definitive diagnostic information, and it is advisable to avoid using such rules in practice as much as possible.

4 Conclusions

In this study, a fuzzy quality abnormality diagnosis model was developed using FRPNs, and a simulation model was created using stateflow. In practical application, the model takes control chart sample data as input, measure the occurrence degree of potential abnormal patterns in control chart, simulate the fuzzy reasoning process of FRPNs, and ultimately provide the potential source of quality anomalies. The diagnosis process and results can be visually demonstrated in a dynamic manner.

The paper's conclusions are as follows:

(1) The simulating model for uncertain abnormality diagnosis is effective, as the elements of stateflow reliably express fuzzy reasoning rules. The simulation results can prioritize the causes of the current abnormality and provide decision support for its elimination.

(2) By assigning occurrence degrees to abnormal patterns associated with rules, the simulating process can validate the correctness of the rules and promptly identify any errors in the model.

(3) When adding new reasoning rules to the simulating model, it is not necessary to construct the entire model. Instead, the new rules can be added based on their corresponding relationships with statement elements.

For the output of the proposed approach, distinct trigger values can be set for different causes. Only when the output exceeds its corresponding trigger value, will the corresponding causes be evaluated. This enables a more effective troubleshooting task. Considering its significant application value, further research is needed to explore the establishment of trigger values based on extensive process data. Since this paper only examined five uncertain abnormal patterns, it is necessary to validate the proposed simulation method with a wider range of patterns.

This research was funded by the Natural Science Foundation of Hunan Province, China, grant number 2022JJ30206 and Research Foundation of Education Bureau of Hunan Province, China, grant number 22A0444.

References

1. T.V. Manoj, J. Leena , R. B.Soney, Knowledge representation using fuzzy Petri nets revisited. *Ieee T Knowl Data En*, **4**, 666-667 (1998)
2. W.M. Wang, X. Peng, G.N. Zhu, J. Hu, Y.H. Peng, Dynamic representation of fuzzy knowledge based on fuzzy petri net and genetic-particle swarm optimization. *Expert Syst Appl*, **4**,1369-1376 (2014)
3. H.Liu, Q. Lin, M. Ren, Fault diagnosis and cause analysis using fuzzy evidential reasoning approach and dynamic adaptive fuzzy Petri nets. *Comput Ind Eng*, **4**, 899-908 (2013)
4. M. Amin, D. Shebl, Reasoning dynamic fuzzy systems based on adaptive fuzzy higher order Petri nets. *Inform Sciences*, **286**, 161-172 (2014)
5. Y.Ye, Z. Jiang, X. Diao, G.t. Du, Extended event-condition action rules and fuzzy Petri nets based exception handling for workflow management. *Expert Syst Appl*, **9**, 10847-10861 (2011)

6. Z. Liu, H. Li, P. Zhou, Towards timed fuzzy Petri net algorithms for chemical abnormality monitoring. *Expert Syst Appl*, **8**, 9724-9728 (2011)
7. M. Vujosevic, M. Dragana, Fuzzy petri net based reasoning for the diagnosis of bus condition. *In Proceedings of 7th Seminar on Neural Network Applications in Electrical Engineering, NEUREL 2004*, 225-229 (2004)
8. R. Daniel, M. Eugenia, Z. Noureddine, Fuzzy Petri nets for monitoring and recovery. *In Proceedings of the 2003 IEEE international conference on Robotics & Automation, Changsha, Hunan, China*, **3**, 4318-4323 (2003)
9. K. Zhou, A. Zain, L. Mo, A decomposition algorithm of fuzzy Petri net using an index function and incidence matrix, *Expert Syst Appl*, **8**, 3980-390 (2015).
10. H. C. Liu, X. Luan, W. Lin, Y. Xiong, Grey reasoning Petri nets for large group knowledge representation and reasoning, *IEEE T Fuzzy Syst*, **12**, 3315-3329 (2019)
11. X. L. Sun, N. Wang, Gas turbine fault diagnosis using intuitionistic fuzzy fault Petri nets. *J Intell Fuzzy Syst*, **6**, 3919-3927 (2018)
12. N. Lu, B. Xu, S. Fang, Research on Fault Diagnosis Simulation of Hydraulic System of CNC Machine Tool Based on Fuzzy Petri Net. *2019 4th International Conference on Power and Renewable Energy (ICPRE)*, IEEE, 201-205 (2019).
13. A. A. Pouyan, M. T. Yadollahzadeh, FPN-SAODV: using fuzzy petri nets for securing AODV routing protocol in mobile Ad hoc network. *Int J Commun Syst*, **1**(2017):e2935. <https://doi.org/10.1002/dac.2935>
14. B. Xu, X. Yin, Fault diagnosis of power systems based on temporal constrained fuzzy petri nets. *IEEE Access*, **7**, 101895-101904 (2019)
15. F. Liu, M. Heiner, D. Gilbert, Fuzzy Petri nets for modelling of uncertain biological systems. *Brief Bioinform*, **1**, 198-210 (2020)
16. Z. Chen, B. Xu, N. Lu, A fault diagnosis method for flexible manufacturing tool system based on fuzzy Petri net. *2019 International Conference on Intelligent Informatics and Biomedical Sciences (ICIIBMS)*, IEEE, Shanghai China, 21-24 (2019)
17. M. Markiewicz, L. Gniewek, A program model of fuzzy interpreted Petri net to control discrete event systems, *Appl Sci*, **4**, 422 (2017)
18. L. Wang, W. Dai, J. Ai, Reliability evaluation for manufacturing system based on dynamic adaptive fuzzy reasoning Petri net. *IEEE Access*, **8**, 167276-167287 (2020)
19. H. Kaid, A. Al-Ahmari, N. Alqahtani, Fault Detection, Diagnostics, and Treatment in Automated Manufacturing Systems Using Internet of Things and Colored Petri Nets. *Machines*, **2**, 173 (2023)
20. E. Kindler, M. Weber, The petri net kernel an infrastructure for building petri net tools, *Int J Softw Tools Te*, **3**, 486-497 (2001)
21. W. Zhang, Z. Salcic, A. Malik, Towards Formal Modelling and Analysis of System J GALS Systems using Coloured Petri Nets. *2019 IEEE 17th International Conference on Industrial Informatics (INDIN) IEEE*, Helsinki, Finland, 152-159 (2019)
22. L. Cabac, M. Haustermann, D. Mosteller, Software development with Petri nets and agents: Approach, frameworks and tool set. *Sci Comput Program*, **157**, 56-70 (2018)
23. J. Dong, J. Jiao, H. Xia, Safety Simulation and Analysis for Complex Systems Concurrency Based on Petri Net and Stateflow Model. *2019 Annual Reliability and Maintainability Symposium (RAMS) IEEE*, Orlando, USA, FL, 1-7 (2019)
24. B. C. Wang, M. Sechilariu, F. Locment, Power flow Petri Net modelling for building integrated multi-source power system with smart grid interaction. *Math Comput Simulat*, **91**, 119-133 (2013)

25. R.Cao, F. Wang, L. Hao, Modeling and simulation of cascade reservoirs flood control system based on hybrid stochastic timed Petri nets. *2016 Chinese Control and Decision Conference (CCDC) IEEE*, 997-1002 (2016)
26. C. Chen, Z. Xing, Y. Xi, Ensuring sufficient cabin hospital beds for curbing the spread of COVID-19—Findings from petri net analysis. *Heliyon*, **10**(2022)e11202. <https://doi.org/10.1016/j.heliyon.2022.e11202>